NANO LETTERS

2004
Vol. 4, No. 4
725−731

Correlating AFM Probe Morphology to Image Resolution for Single-Wall Carbon Nanotube Tips

Lawrence A. Wade,[†,‡] Ian R. Shapiro,[§] Ziyang Ma,[‡] Stephen R. Quake,[‡] and C. Patrick Collier*[,§]

Jet Propulsion Laboratory and Departments of Applied Physics and Chemistry, California Institute of Technology, Pasadena, California 91125

Received January 2, 2004; Revised Manuscript Received January 31, 2004

ABSTRACT

Scanning and transmission electron microscopy were used to image hundreds of single-wall carbon nanotube probes and to correlate probe morphology with AFM image resolution. Several methods for fabricating such probes were evaluated, resulting in a procedure that produces image-quality single-wall nanotube probes at a rate compatible with their routine use. Surprisingly, about one-third of the tips image with resolution better than the nanotube probe diameter and, in exceptional cases, with resolution better than 1 nm. This represents the highest lateral resolution reported to date for a SWNT probe.

Single-wall carbon nanotubes (SWNTs) have shown great potential as high-resolution AFM imaging probes.[1−3] The level of resolution possible for both single molecule imaging and force transduction in AFM is ultimately limited by the structure of the tip. Commercially available silicon probe tips have radii of curvature of 5−15 nm. The finest commercially available Si tips are very delicate, leading to substantial variation in tip shape and size even between successive images. SWNTs, on the other hand, have diameters between 1.5 and 6 nm, providing resolution comparable to molecular scale dimensions. Carbon nanotubes are chemically and mechanically robust, with axial Young's moduli of about 1.25 TPa,[4,5] resulting in a tip structure that is stable over prolonged imaging periods.[6] Finally, SWNTs can be chemically functionalized uniquely at their very ends, permitting a broad array of applications in nanotechnology and biotechnology.[7] Nevertheless, it is difficult to reproducibly assemble large quantities of high-quality single-wall nanotube AFM tips. To fully realize the promise of these probes for high-resolution AFM, a better physical understanding is needed of how the geometry of the mounted SWNT on its AFM tip support affects image quality.

Successfully fabricating a probe suitable for AFM imaging in air involves several steps: attaching the nanotube to a silicon AFM tip, shortening it sufficiently to enable high resolution imaging, characterizing its quality, and storing it for later use. Building upon previously reported techniques, we have conducted a comparative survey of fabrication methods to produce a protocol that routinely results in high quality probes. The quality of the AFM images taken with the resultant probes, along with the frequency and ease of success, was used to distinguish between the several approaches studied. In addition, SEM and TEM images of hundreds of nanotube AFM probes were used to evaluate the efficacy of different probe attachment and shortening techniques and to improve the accuracy of our interpretation of AFM imaging and force calibration results. For the first time, the AFM resolution achieved when imaging with nanotube probes was directly correlated to TEM images taken of these same probes. This allowed us to carry out a rigorous examination of nanotube morphology and its influence on image resolution and quality, by directly correlating nanotube geometry, as determined with TEM imaging, with their performance as AFM probes. As a result, we gained significant new insights that are important for research groups performing AFM imaging with SWNT tips.

In this paper, we summarize the results of these studies and describe a procedure that enables consistently successful nanotube probe fabrication. The lateral resolution of these probes when used to image 3 nm diameter SWNTs was typically less than 4 nm, and in one case, 5 Å.[8] This is an improvement by a factor of 4 over the best resolution reported to date using a SWNT probe, which is 2.0 nm.[9] The systematic correlation of TEM images of SWNT probes with the effective lateral resolution obtained when using these probes for topographical imaging indicates that approxi-

* Corresponding author. E-mail: collier@caltech.edu.
† Jet Propulsion Laboratory.
‡ Department of Applied Physics.
§ Department of Chemistry.

10.1021/nl049976q CCC: $27.50
Published on Web 02/17/2004

mately one-third of the probes demonstrated resolution smaller than the diameter of the nanotube probe itself when imaging nanotubes on a smooth substrate. For example, we have measured 1.2 nm lateral resolution from a SWNT scanning probe that was 5.5 nm in diameter.

These TEM−AFM correlations provide experimental evidence consistent with previous mechanical modeling carried out by Snow, et al.[10] Additionally, whereas previous investigations have shown nanotube buckling to be an elastic process,[2,3,9,11] we have found that under some circumstances, a SWNT probe can buckle inelastically, resulting in probe damage and corresponding image artifacts.

Finally, we have found that nanotubes picked up by AFM tips can have larger diameters (by about a factor of 2) than the diameters of nanotubes imaged on the surface of the growth substrate, as determined from height measurements with a conventional AFM tip. A better understanding of this discrepancy is needed for optimizing the yield and reproducibility of nanotube probe fabrication. The AFM image resolution statistics we report here underscore the variability between probes fabricated by different methods.

Digital Instruments BioScope and Multimode atomic force microscopes were used with Nanoscope IV controllers for this work. Transmission electron microscopy was performed with a Phillips EM430, and scanning electron microscopy was performed with a Hitachi 4100.

We compared several methods for attaching nanotubes to silicon AFM tips: manual assembly, direct growth, and pickup. Smalley's group reported the first example of the use of carbon nanotubes as AFM tips in 1996.[11] Manual assembly of AFM probes was found to be relatively simple, although the nanotubes had to be large enough to be seen and manipulated under an optical microscope, and thus did not yield high-resolution probes. While direct growth[12−14] offers the potential for parallel fabrication of SWNT AFM probes, we found that the yield was quite low. We also determined that the rate-limiting step in probe fabrication was the nanotube shortening step rather than attachment. Therefore, we focused our efforts on the pick-up technique for nanotube attachment, as shown in Figure 1.

The pick-up technique, developed by Lieber et al.,[15] is an efficient and consistent method for mounting SWNTs in the proper orientation. When SWNTs are grown on a flat substrate, a small percentage of the tubes are oriented vertically, and can be picked up when the AFM tip scans across the surface in tapping mode. The nanotube binds to the side of the pyramidal AFM tip via attractive van der Waals forces, and usually remains attached firmly enough that it can be repeatedly pressed into and scanned across the substrate surface. We found that it was important to reduce the field of view (e.g., from 10 μm to 10 nm) or retract the tip as soon as a nanotube was successfully picked up in order to minimize the probability of picking up additional nanotubes (see Supporting Information). Multiple attached tubes or bundles can lead to AFM image artifacts.

It is also important to note that the ambient humidity appears to affect the efficiency of the pickup method. We found it nearly impossible to pick up nanotubes from a substrate under high humidity conditions. Enclosing the AFM in a glovebag under a flow of dry nitrogen for about 30 min rejuvenated the process. We speculate that an increase in the relative humidity makes it more difficult to pick up nanotubes for two main reasons. First, at higher humidity values, it is harder to overcome capillary forces due to the build up of a surface layer of water on the growth substrate. More force is necessary to pry a prone nanotube off the surface due to increased adhesion. Second, increasing water build up on the tip decreases the attractive interactions of the nanotube to the silicon surface of the AFM tip during pick up. It is known that the van der Waals interactions at the nanotube−AFM tip interface are not strong enough to keep the tube attached to the tip in liquid water.[9] Nanoscopic condensation of water between the AFM tip and the growth substrate at high relative humidity may have an analogous effect on the success rate for picking up a nanotube.

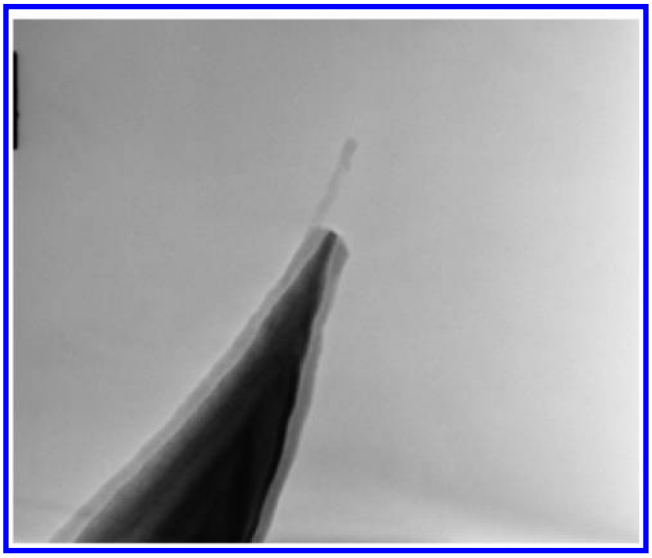

Figure 1. TEM image of a single-wall carbon nanotube picked up from a silicon substrate.

SWNTs were grown via chemical vapor deposition (CVD) on 4 mm to 8 mm square, 500 μm thick p-doped Si wafers. Four different methods were used to coat the substrates with iron catalyst for growing nanotubes suitable for pickup: spin coating a solution of $Fe(NO_3)_3 \cdot 9H_2O$ in isopropyl alcohol,[9] thermal evaporation of iron onto the substrate, electron beam evaporation of iron onto the substrate,[15] and incubation with ferritin. We achieved the most uniform deposition of small (1−2 nm) catalytic sites with high spatial density by using ferritin-derived iron nanoparticles, prepared as described by Dai and co-workers.[16]

CVD growth was performed in a 22 mm inner diameter Lindberg/Blue M quartz tube furnace with a single heating zone 312 mm long, as shown in Figure 2. Five wafers are positioned 12.5 mm apart in a specially designed quartz holder, oriented vertically and with the catalyst-coated side facing away from the direction of the incoming gas. A significant advantage of this holder is that it enables up to three small substrates to be mounted side-by-side in each slot for parallel comparison of growth results under nearly identical temperature and gas flow conditions.

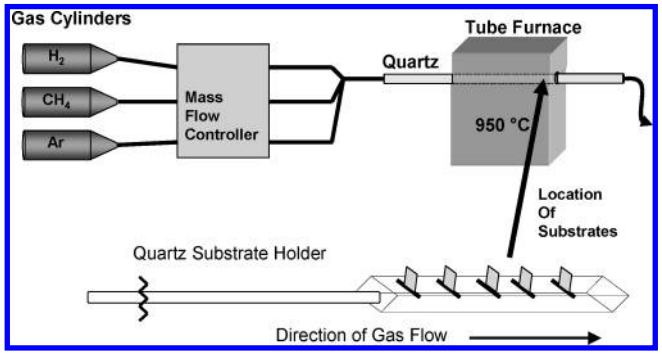

Figure 2. Diagram of CVD apparatus for production of nanotube substrates.

We found that growth was faster (5 μm long nanotubes within one minute) and the distribution of tube lengths increased when the catalyst-coated surface was facing away from the incoming gas flow. We speculate that this is due to increased turbulence of the gas flow at the catalyst coated side after passing over the edges of the substrate. Induced turbulence should minimize the role of diffusion-limited growth relative to nucleation rate in the growth kinetics, but at the expense of uniform growth. These growth procedures generate SWNTs on the substrate with diameters ranging from 1.6 to 3.0 nm, and lengths between 100 nm and 5 μm, as imaged with AFM and SEM.

The distribution of tube diameters varied with the size of the catalytic sites. For example, we found that spin coating many drops of dilute solution of the iron nitrate catalyst to give a high density of small catalytic sites gave a slightly broader tube diameter distribution than did ferritin. In contrast, depositing a few drops of higher density iron solutions yielded broad size distributions and larger average tube diameters. Based on AFM analyses of these substrates, it appears that the larger tube diameters resulted from larger catalytic sites on the substrate. No MWNTs have been observed on these substrates.

The long-term stability of pickup substrates appears to vary depending on how they were prepared. Ferritin and ferric nitrate substrates appear to be substantially less effective for pickup attachment after 4 to 6 months. We hypothesize that this is due to the relatively weak mechanical attachment of the catalytic site to the substrate. Over time, vertically oriented tubes that are attached to loosely bound catalytic sites apparently physisorb onto the substrate. Enclosing the AFM in a glovebag with a flow of dry nitrogen for about 30 min substantially enhanced pickup with these older substrates. In contrast, substrates that had the catalytic sites deposited by molecular beam epitaxy (MBE) have demonstrated reliable pickup of nanotubes with an AFM tip over several years without special care.[15]

The diameters of the picked up tubes measured with TEM were typically between 4 and 6 nm. In comparison, the diameters of nanotubes lying horizontally on the substrate, determined by AFM height measurements, were only 2−3 nm. We have ruled out TEM and AFM calibration errors as the cause of this discrepancy. We have also ruled out compression of the imaged nanotubes by the AFM tip, which would result in a decreased apparent diameter. Deformation of the horizontal nanotubes due to van der Waals forces has also been modeled using realistic molecular dynamics simulations based on quantum mechanical calculations, and found insufficient to explain this discrepancy.[17] It appears that this disparity is real and not just an artifact due to tube distortion or measurement error.

This indicates a strong preference for larger diameter tubes to be picked up by silicon AFM probes. There are two plausible explanations for this disparity. One possibility is that larger diameter nanotubes have a higher probability of remaining vertically oriented on the growth substrate over time than smaller diameter tubes. Only the population of smaller diameter nanotubes adsorbed to the growth substrate can be imaged by AFM. Hence, AFM images will be biased toward this part of the distribution of nanotube diameters.

Alternatively, this disparity may be explained by the binding energy of the nanotube to the AFM cantilever tip relative to the binding energy of the nanotube to the substrate. Once a SWNT has been picked up by a scanning AFM tip, there are two kinds of motions that impose stress on the system. The AFM cantilever has a net motion parallel to the substrate. During pick-up, typical horizontal velocities are on the order of 30 000 nm/s. This motion imposes three kinds of stress on the system: shear, bending, and tension. In addition, the cantilever has a rapid vertical oscillation, typically 70−250 kHz, with an amplitude of 40−50 nm, that imposes additional bending and tension stresses.

The mechanical stresses imposed by the cantilever motion on a nanotube attached on one end to the AFM tip, and on the other end to the surface of the growth substrate, will result in one of two outcomes: the nanotube either slips off the cantilever tip and remains attached to the substrate, or the nanotube separates from the substrate interface and is "picked up". The discriminator between these two outcomes is the binding energy at the attachment site of the nanotube to the silicon tip relative to that of its attachment to the substrate. These binding energies will depend on many factors that are virtually impossible to characterize fully, such as the relative lengths of the nanotube adsorbed onto the tip versus the substrate, as well as details of the chemical, physical, and mechanical interactions between the nanotube and these surfaces during scanning in tapping mode. It is known, however, that binding energy scales with the tube diameter, which can be determined directly from both AFM and TEM images.

The strength of nanotube attachment can be approximated as being linearly proportional to the nanotube diameter using the thin-walled cylinder approximation. At the attachment site with the AFM cantilever tip, the nanotube can be considered fixed until the binding energy is exceeded at this interface by the imposed stresses. This binding force increases linearly with diameter, but at a rate 1.6 times faster for tubes greater than 2.7 nm diameter than it does for smaller diameter nanotubes.[18] The increased binding energy for nanotubes greater than 2.7 nm could result in larger diameter nanotubes being preferentially picked up. The relative adhesion strength of the catalytic particle to the tube versus

the substrate could also have a significant influence on the diameters of the tubes that are picked up.

As seen in Figure 1, more than 100 nm of a nanotube typically protrudes from the end of the AFM tip after pick-up. High-resolution imaging is not possible with such a long nanotube tip due to thermal fluctuations and bending. Pick-up SWNT tips were shortened by a combination of push shortening, an approach developed by Hafner and Lieber,[13] and electrical pulse etching.[2,12] An HP 8114A pulse generator was used in combination with a Digital Instruments signal access module for all of our pulse shortening experiments.

Push shortening is done by incrementally decreasing the tip−sample separation distance during successive force calibrations to push the nanotube up along the side of an AFM tip. This process requires a picked-up tube of very specific length. Tubes longer than 100 nm tend to buckle inelastically during this process, after which they cannot be shortened by further pushing. Push shortening is superior to pulse etching when further shortening nanotubes less than 100 nm long in very small increments.

We obtain similar results for electrical pulse etching with native oxide coated p-doped silicon, 300 nm thick thermally grown oxide-coated p-doped silicon, and gold-plated silicon substrates. This finding indicates that the entire probe fabrication procedure can be carried out on a single unpatterned, doped-silicon substrate. Thermally grown oxide substrates typically required higher voltages to successfully pulse-shorten than did either native oxide or gold-coated silicon substrates.

Using electrical pulse shortening and push shortening in combination on the same tip relaxes the constraints for obtaining high-quality probes from the nanotube growth substrate and increases yield. Long tubes can be coarsely shortened with electrical pulses until their lengths are less than 100 nm. Push shortening can then be used for finer control in adjusting the probe length.

We frequently found that electrostatic forces would strip nanotubes off the AFM tips when they had been stored in a nonconductive container. An aluminum box with a narrow strip of double-sided tape or a conductive Gel-Pak container both seemed to solve this problem. Prior to use of conductive boxes for nanotube tip storage, we were unsuccessful in TEM imaging the attached nanotube probes.

To characterize the effective resolution of our SWNT probes, we imaged nanotubes resting flat on the silicon growth substrate, using a scanning field of view of 100−350 nm. We define resolution as the full width of the imaged tube measured at the noise floor, minus the measured tube height. While nanotubes are convenient samples for determining resolution, they are not infinitely rigid. Dekker's group has shown that the apparent height of a nanotube measured by tapping mode imaging can decrease substantially at high oscillation amplitudes, even with conventional silicon tips.[19] We have observed similar effects with nanotube probes.[20] For this study, the oscillation amplitude was maintained close enough to its freely oscillating value in air to limit this effect to be within 10% of the true nanotube height.

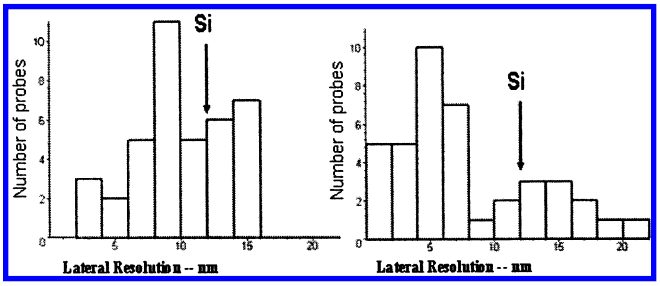

Figure 3. The left histogram summarizes the resolution for 39 probes fabricated on a substrate coated with ferric nitrate catalyst. The right histogram shows the resolution distribution of 40 probes made from nanotubes picked up from a substrate coated with ferritin. Included is the typical resolution obtainable with a conventional silicon AFM tip.

Figure 3 shows histograms of the lateral resolutions obtained with SWNT probes fabricated using a growth substrate coated with ferric nitrate catalyst versus those fabricated using ferritin as the catalyst. The variation in nanotube probe performance was greater than we expected based on previous reports. Leiber et al. had examined the image quality of different nanotube types (MWNTs and SWNTs).[21] In contrast, we compared 39 SWNTs made from the same iron nitrate-coated substrate and 40 from a ferritin substrate. The wide range in resolution found, between the two different kinds of substrate (ferritin vs iron nitrate), as well as from the same substrate, was surprising and underscores the importance of specific nanotube characteristics in determining the maximum achievable resolution.

There is a clear shift in the distribution toward higher resolution probes when ferritin was used as the catalyst, consistent with a narrower catalyst size distribution. It is not clear how much technique improvements rather than the switch to ferritin from ferric nitrate coated substrates played in the comparative distribution. Most of the latter tips were fabricated using ferritin substrates. By that time, we were more careful to reduce the field of view immediately after pick-up to minimize bundle formation. This could explain why there are fewer 10−15 nm resolution tips. However, it is clear that significantly more probes with resolution better than 5 nm were fabricated using ferritin substrates.

Nearly 100 probes were imaged by TEM to characterize the efficacy of different fabrication techniques. Of these, fourteen SWNT probes imaged by TEM had previously been used for tapping-mode topographic imaging. Table 1 presents a summary of probe characteristics determined by TEM−AFM correlations for the fourteen SWNT probes. Entries in bold correspond to probes that demonstrated lateral resolution less than the actual nanotube probe diameter.

Image quality is a function of many factors including: tube diameter and length, contact angle, number of nanotubes extending past the silicon tip, thermal noise, and contamination. These factors can lead to substantial variability in resolution. By correlating probe structure and orientation seen in the TEM images with topographic imaging performance, we can provide experimental evidence consistent with previous mechanical modeling carried out by Snow et al.,[10] who have shown that lateral tip−sample forces can bend

Table 1. TEM−AFM Correlation Table for Single-Wall Carbon Nanotube Scanning Probes

tip type	tube diameter	tube length	aspect ratio	deviation from perpendicular	lateral resolution (full width-height)	lateral resolution/ probe diameter
SWNT	**4.2 nm**	**10 nm**	**2.4**	**10°**	**2.8 nm**	**0.67**
Bundle	**9.3 nm**	**77 nm**	**8.3**	**20°**	**4.0 nm**	**0.43**
SWNT	4.0 nm	112 nm	28	30°	10.4 nm	2.60
SWNT[a]	4.0 nm	19 nm	4.8	40°	4.6 nm	1.15
SWNT	**5.5 nm**	**40 nm**	**7.3**	**20°**	**1.2 nm**	**0.22**
Bundle	**8.0 nm**	**35 nm**	**4.4**	**15°**	**5.6 nm**	**0.70**
SWNT	3.7 nm	30 nm	8.1	30°	5.8 nm	1.56
SWNT[a,b]	4.2 nm	33 nm	7.9	20°	6.0 nm	1.43
SWNT	5.4 nm	38 nm	7.0	10°	5.9 nm	1.09
SWNT	3.5 nm	15 nm	4.3	20°	4.4 nm	1.26
Bundle	5.5 nm	51 nm	9.3	0°	21 nm	4.0
SWNT	**5.3 nm**	**55 nm**	**10.4**	**0°**	**3.9 nm**	**0.74**
SWNT	**6.5 nm**	**42 nm**	**6.5**	**0°**	**4.3 nm**	**0.66**
SWNT	5.4 nm	26 nm	4.8	10°	8.0 nm	1.48

[a] Probe showed a "shadowing" artifact. [b] Nanotube appeared buckled 16 nm from the end of the tube.

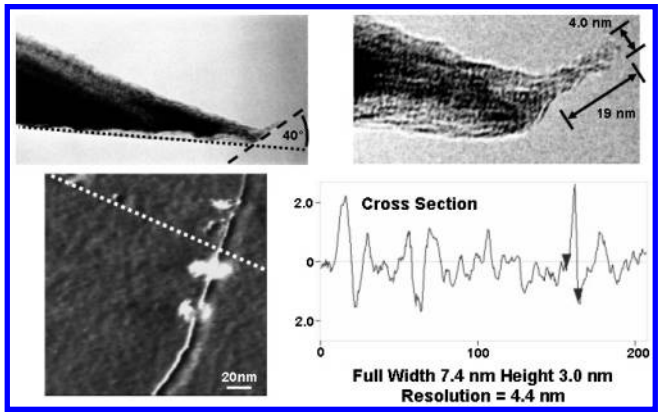

Figure 4. Correlation of image showing artifact due to large contact angle with substrate. Additionally, this nanotube appears to be buckled near the silicon tip. The dotted black line in the upper left image is perpendicular to the substrate.

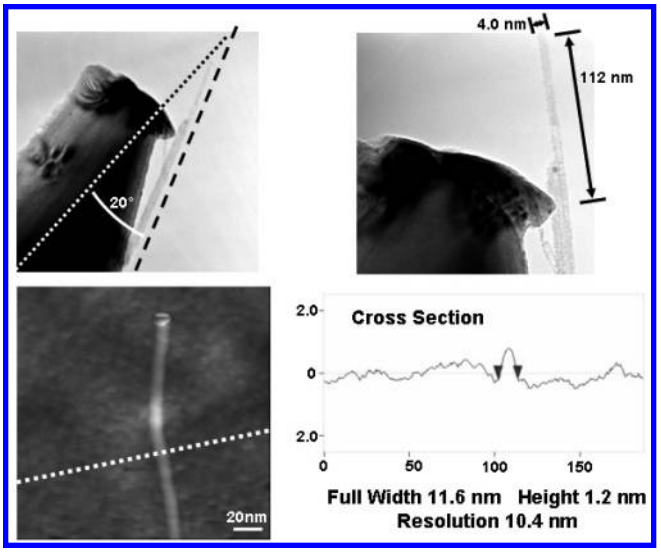

Figure 5. Image artifacts due to bending are significant for long nanotubes. Note that there are a number of picked up nanotubes at the base of this tip. The damage to the silicon tip probably occurred during repeated force calibrations.

single-wall nanotubes or cause snap-to-contact behavior when the tubes exceed either a critical length or a critical angle relative to the substrate surface normal. These effects introduce a significant degree of broadening and the appearance of image artifacts.

If the nanotube is presented to the sample surface at an angle deviating from the surface normal by more than ∼30°, poor resolution and obvious image artifacts result due to tip−sample forces having a significant component perpendicular to the nanotube axis. For example, Figure 4 shows a 19 nm long, 4 nm diameter nanotube projecting from the probe tip at an angle of 40°. This probe produced an image that contained a positive height "shadowing" artifact approximately 10 nm in width parallel to each sample nanotube. This artifact resulted from the nonideal orientation of the probe. Additionally, the TEM image showed that the nanotube is buckled near the silicon tip. Previous reports have described reversible *elastic* buckling of the nanotube, which did not have a serious impact on image quality.[5,9,21] Our TEM correlations indicate, however, that buckling can, under some circumstances, be inelastic, resulting in irreversible structural changes. This structural defect results in an effectively lower stiffness for the probe, which we believe is responsible for the decreased resolution and imaging artifacts we observe (shadowing features). Similar artifacts were seen with SWNT ropes (multiple SWNTs bundled together) for the same reason; the layered structure of a bundle of nanotubes attached to the AFM tip results in stiffness variation along the probe length.

SWNTs must also have aspect ratios less than ∼10 to be adequate for imaging purposes. Figure 5 shows a 4 nm diameter nanotube protruding 112 nm from the end of the AFM tip, but at an angle deviating from the surface normal by less than 20°. The resulting lateral resolution was still 2.5 times the probe tube diameter. This broadening of the image is due in small part to thermal vibrations. However, mechanical modeling studies have indicated that for a nanotube of this geometry, the root-mean-squared thermal vibrations of the end of the tube should be less than 2 Å.[22] Nanotube bending due to lateral tip−sample forces is most likely the principal contribution to the degraded resolution.

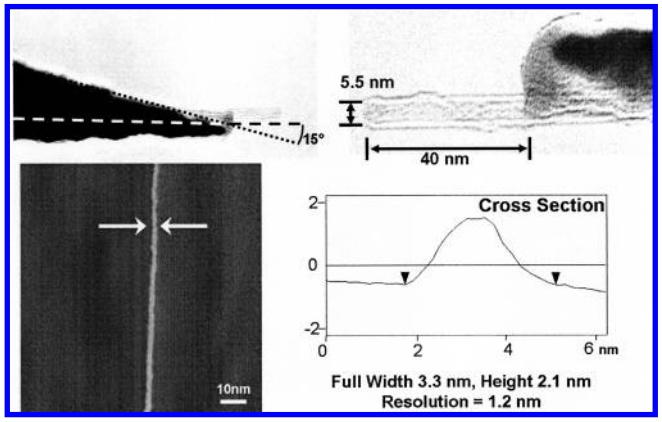

Figure 6. TEM−AFM correlation of a SWNT probe that demonstrated an effective lateral resolution that was 22% of the probe diameter.

Images taken with high quality nanotube probes show no sign of artifacts. These probes all had the nanotubes oriented on the tip at angles close to the substrate surface normal (within 10−20°) and had protrusion lengths ≤40 nm. By directly measuring the nanotube width from each TEM image and comparing that to the obtained AFM resolution, we have determined the average ratio of AFM resolution to tube diameter for SWNT probes in this class to be 1.17. This is a reasonable value, given that thermal vibrations and bending of the nanotube will always slightly increase its effective imaging diameter.

In about 1/3 of the high quality nanotube probes made from the ferritin substrate, as shown in Figure 6, it was found that the effective lateral resolution was significantly *better* than the nanotube probe diameter measured directly with TEM. Figure 6 shows a nanotube probe 5.5 nm in diameter that demonstrated a lateral resolution of 1.2 nm, just 22% of the diameter of the nanotube. It is likely that this enhanced resolution occurs when the nanotube contacts the substrate being imaged with either an asperity or at a specific angle such that only an edge of the nanotube is in contact with the substrate. Imaging a small object with an asperity or an open edge of the tube could lead to the high resolutions observed. Molecular dynamics simulations of surface−nanotube and nanotube−nanotube interactions indicate that other phenomena may also be important, including elastic deformation of the sample nanotube relative to the probe nanotube.[17]

In conclusion, we have combined elements from several previously reported techniques for producing nanotube tips suitable for AFM imaging dry samples that significantly reduce the time of manufacture while improving reproducibility and performance. Feedback from SEM and TEM images of the nanotube probes was used to directly evaluate the effectiveness of the different techniques employed for each of the steps in the fabrication procedure. The optimal process involves the following six steps. (1) Grow nanotubes from ferritin-derived iron nanoparticles on conductive silicon substrates coated only with its native oxide. (2) Pick up a SWNT by imaging the substrate with a 10 μm field of view in tapping mode. (3) Quickly reduce the field of view to approximately 10 nm so that additional tubes are not picked up. (4) Shorten the tube to an appropriate length for imaging without changing substrates using a combination of electrical pulse and push shortening techniques. (5) Image a 100−500 nm region of the substrate to characterize the probe quality. (6) Store shortened nanotube probe in a conductive box.

By growing nanotubes directly on a conductive p-doped silicon substrate with only a native oxide layer, it is possible to pick up, shorten, and test the probe resolution without having to switch samples. This proved to be a significant timesaving optimization. We have found that the resulting nanotube growths (diameter and length) are very similar for all of the investigated catalyst deposition techniques if the spatial density and diameters of catalytic sites are similar. Rates of production have typically reached one probe per hour for several consecutive hours. On exceptional days, the rate can be as high as several per hour. This success has been duplicated with incoming group members.

Overall, we have found AFM image quality to be consistently and significantly better with nanotube tips than with the best silicon AFM tips. Correlations of TEM images of SWNT probes with the effective lateral resolution obtained when using these probes for topographical imaging with AFM indicate that approximately one-third of the probes demonstrate resolution better than the diameter of the nanotube probe itself when imaging nanotubes on a smooth substrate. The methodology described here has resulted in a sufficiently high level of productivity to enable development of single-molecule probes and sensors using functionalized nanotube tips, and has proven capable of fabricating AFM probes with the highest resolution reported to date.

Acknowledgment. The authors thank Jason Hafner, Jim Hone, and Jordan Gerton for fruitful discussions and suggestions. We also thank Carol Garland for many patient hours of TEM imaging and NanoDevices, Santa Barbara, CA for providing direct growth nanotube tips for characterization. Wade, Ma, and Quake were supported by a grant from Pharmagenomix; Shapiro and Collier were supported by Caltech startup funds. Wade, Shapiro, and Collier were also supported by the Caltech President's Fund and NASA contract NAS7-1407.

Supporting Information Available: Experimental procedures for SWNT growth and AFM probe fabrication. This material is available free of charge via the Internet at http://pubs.acs.org.

References

(1) Hafner, J. H.; Cheung, C.-L.; Wooley, A. T.; Lieber, C. M. *Prog. Biophys. Mol. Biol.* **2001**, *77*, 73.
(2) Wong, S. S.; Harper, J. D.; Lansbury; P. T., Jr.; Lieber, C. M. *J. Am. Chem. Soc.* **1998**, *120*, 603.
(3) Wong, S. S.; Woolley, A. T.; Odom, T. W.; Huang, J. L.; Kim, P.; Vezenov, D. V.; Lieber, C. M. *Appl. Phys. Lett.* **1998**, *73*, 3465.
(4) Krishnan, A.; Dujardin, E.; Ebbesen, T. W.; Yianilos, P. N.; Treacy, M. M. J. *Phys. Rev. B* **1988**, *58*, 14013.
(5) Wong, E. W.; Sheehan, P. E.; Lieber, C. M. *Science* **1997**, *277*, 1971.
(6) Larsen, T.; Moloni, K.; Flack, F.; Eriksson, M. A.; Lagally, M. G.; Black, C. T. *Appl. Phys. Lett.* **2002**, *80*, 1996.
(7) Wong, S. S.; Joselevich, E.; Wooley, A. T.; Cheung C.-L.; Lieber, C. M. *Nature* **1998**, *394*, 52.

(8) Wade, L. A.; Shapiro, I. R.; Ziyang, M.; Quake, S. R.; Collier, C. P. *Nanotech 2003* **2003**, *3*, 317.
(9) Hafner, J. H.; Cheung, C.-L.; Oosterkamp, T. H.; Lieber, C. M. *J. Phys. Chem. B* **2001**, *105*, 743.
(10) Snow, E. S.; Campbell, P. M.; Novak, J. P. *Appl. Phys. Lett.* **2002**, *80*, 2002.
(11) Dai, H.; Hafner, J. H.; Rinzler, A. G.; Colbert, D. T.; Smalley, R. E. *Nature* **1996**, *384*, 147.
(12) Cooper, E. B.; Manalis, S. R.; Fang, H.; Dai, H.; Minne, S. C.; Hunt, T.; Quate, C. F. *Appl. Phys. Lett*. **1999**, *75*, 3566.
(13) Hafner, J. H.; Cheung, C. L.; Lieber, C. M. *J. Am. Chem. Soc.* **1999**, *121*, 9750.
(14) Hafner, J. H.; Cheung, C.-L.; Lieber, C. M. *Nature* **1999**, *398*, 761.
(15) Hafner, J.; Rice University, private communication, March, 2002.
(16) Li, Y.; Kim, J. W.; Zhang, Y.; Rolandi, M.; Wang, D.; Dai, H. *J. Phys. Chem. B* **2001**, *105*, 11424.
(17) Shapiro, I. R.; Solares, S.; Esplandiu, M. J.; Wade, L. A.; Quake, S. R.; Goddard, W. A.; Collier, C. P., manuscript in preparation.
(18) Hertel, T.; Walkup, R. E.; Avouris, Ph. *Phys. Rev. B* **1998**, *58*, 13870.
(19) Postma, H. W. C.; Sellmeijer, A.; Dekker, C. *Adv. Mater.* **2000**, *12*, 1299.
(20) Esplandiu, M. J.; Shapiro, I. R.; Solares, S.; Matsuda, Y.; Goddard, W. A.; Collier, C. P., manuscript in preparation.
(21) Cheung, C. L.; Hafner J. H.; Lieber, C.; M. *Proc. Natl. Acad. Sci. U.S.A.* **2000**, *97*, 3809.
(22) Yakobson, B. I.; Avouris, Ph. *Topics Appl. Phys.* **2001**, *80*, 287.

NL049976Q